

Thermodynamic Properties of Liquid Silver-Antimony-Tin Alloys Determined from Electrochemical and Calorimetric Measurements

JOANNA ŁAPSA¹ and BOGUSIAW ONDERKA^{1,2}

1.—Faculty of Non-Ferrous Metals, AGH University of Science and Technology, 30 Mickiewicza Ave, 30-059 Krakow, Poland. 2.—e-mail: onderka@agh.edu.pl

The thermodynamic properties of liquid Ag-Sb-Sn alloys were obtained through use of the drop solution calorimetric method and electromotive force (emf) measurements of galvanic cells with a yttria stabilized zirconia (YSZ) solid electrolyte. The experiments were carried out along $\text{Ag}_{0.25}\text{Sb}_{0.75}$, $\text{Ag}_{0.5}\text{Sb}_{0.5}$ and $\text{Ag}_{0.75}\text{Sb}_{0.25}$ sections of the ternary system in the temperature range from 973 K to 1223 K. From the measured emf, the tin activity in liquid solutions of Ag-Sb-Sn was determined for the first time. The partial and integral enthalpy of mixing were determined from calorimetric measurements at two temperatures. These measurements were performed along two cross-sections: $\text{Sb}_{0.5}\text{Sn}_{0.5}$ at 912 K and 1075 K, and $\text{Ag}_{0.75}\text{Sb}_{0.25}$ at 1075 K. Both experimental data sets were used to find ternary interaction parameters by applying the Redlich–Kister–Muggianu model of the substitutional solution. Consequently, the set of parameters describing the thermodynamic properties of the liquid phase was derived.

Key words: Thermodynamics, ternary system, silver alloys, enthalpy of mixing, galvanic cell, tin activity

INTRODUCTION

The Ag-Sb-Sn system has been introduced as a promising lead-free alloy substitute for a high-temperature (melting $T_f \approx 553$ K) Pb-Sn solder, used as a solder interconnect material.¹ Currently, several alloys based on this system are available as commercial solders, e.g., J-Alloy (65Sn-25Ag-10Sb, mass%), which displays good creep resistance.²

Knowledge of the thermodynamic properties of a solder system is important for understanding the soldering process as well as the final reliability of the joints. The Ag-Sb, Ag-Sn, and Sb-Sn binary systems have already been thermodynamically assessed.³ As far as the ternary system is concerned, literature data for the Ag-Sb-Sn system are rather scarce. However, all authors agree that no ternary intermetallic compounds were observed in the Ag-Sb-Sn system.

Gather et al.⁴ determined the heats of mixing of the Ag-Sb-Sn ternary system along four sections at 1224 K and one section at 1253 K using a heat flow calorimeter. Calorimetric studies were also carried out by Li et al.⁵ along five sections at three different temperatures, 803 K, 873 K, and 903 K, using a high-temperature Calvet type calorimeter. They also performed several differential scanning calorimeter (DSC) measurements on the key-composition alloys to determine the temperatures of the invariant reactions.⁵

The liquidus surface and the invariant reactions of the Ag-Sb-Sn system were determined by Masson and Kirkpatrick² and by Chen et al.⁶ using differential thermal analysis combined with metallographic analysis. Cheng and Lee⁷ analyzed phase equilibria in the Ag-rich corner by the metallographic method and x-ray diffraction (XRD) and revealed the Ag-Sb-Sn isothermal section at room temperature. This section was also reported one year later by Zheng et al.⁸ The isothermal sections

(Received November 18, 2015; accepted May 3, 2016; published online May 31, 2016)

at 493 K and at 523 K were reported by Oberndorff et al.⁹ and by Chen et al.,⁶ respectively. Lin et al.¹⁰ determined the isothermal sections at 423 K and 673 K.

Oh et al.¹¹ thermodynamically assessed the Ag-Sb-Sn system, taking into account available thermodynamic and phase equilibria information. However, the calculated results are not consistent with the experimental data obtained by Chen et al.^{6,12} and Masson and Kirkpatrick.² After a thorough literature review, Schmid-Fetzer et al.¹³ proposed a modification of the Oh's solidification diagram, changing the invariant reaction P1 to the invariant reaction of U-type ($U_2: L + \beta \leftrightarrow \epsilon + Sn_3Sb_2$). He noticed that Oh's P₁ reaction ($L + \beta + \epsilon \leftrightarrow Sn_3Sb_2$)¹¹ cannot be correct, since the composition of Sn_3Sb_2 is not located in the tie-line triangle formed by the other three phases. Such a U_2 reaction was confirmed at the temperature 587 K by Chen et al.⁶ by DSC analysis.

Recent assessment of the Ag-Sb-Sn system made by Gierlotka¹⁴ was based on Chen's experimental data,^{6,12} which suggested that the Sn_3Sb_2 phase is stable down to room temperature. Nevertheless, new critical reinvestigation of Sn_3Sb_2 stability⁵ supported the version given by Massalski et al.,¹⁵ which indicates that during temperature decrease the Sn_3Sb_2 phase decomposes into (Sn) and β -SnSb phases. However, despite all these efforts, no activity data for liquid alloys are available in the literature, at least so far. Therefore, the main aim of this work was first of all to complete the thermodynamic data on tin activity in liquid solutions of the Ag-Sb-Sn system by using the emf measurements of the galvanic cell with a zirconia solid electrolyte. Also, to check the consistency of the data, the partial and integral mixing enthalpies of liquid Ag-Sb-Sn alloys were determined by the use of the drop solution calorimetric method along two cross-sections. To our knowledge this is the first time that the tin activity in liquid Ag-Sb-Sn solution has been determined.

METHODS AND MATERIALS

Emf Technique

The ternary alloy samples were prepared from pure silver and tin (99.99 mass%) obtained from POCh (Poland), while the antimony lumps (>99.5 mass%) were delivered by Fluka AG (Switzerland). The powdered tin oxide, SnO_2 , of purity 99.9 mass% was obtained from Sigma-Aldrich (Germany). Ternary silver-tin-antimony samples were alloyed from pure metals of weighed amounts in vacuum-sealed quartz tubes. The alloys were prepared by heating sealed silica ampoules in the resistance furnace and homogenizing samples at 1073 K over about 12 h.

A schematic representation of the cell assembly is shown in Fig. 1. The one-end closed solid yttria stabilized zirconia (YSZ) electrolyte tubes (length

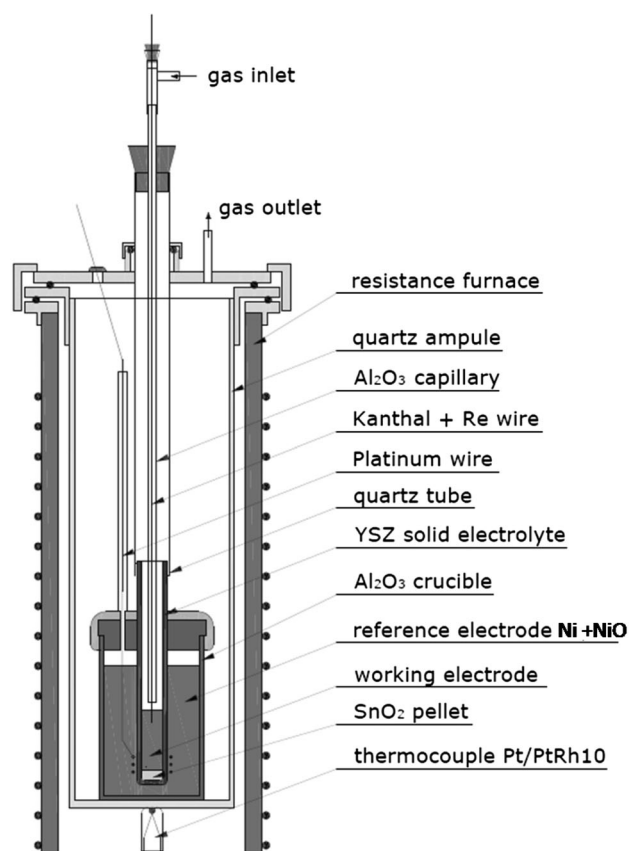


Fig. 1. The galvanic cell assembly.

50 mm, OD/ID = 8/5 mm) were supplied by the Yamari Trading (Japan). The YSZ electrolyte tube contained about 2 g of metallic alloy of chosen composition. Additionally, a small chunk of pelleted SnO_2 powder was placed at the bottom of YSZ tube to assure Sn- SnO_2 equilibrium.

The Kanthal wire with a welded rhenium wire tip, kept inside the alumina tube shield, acted as an electric contact with a liquid metal electrode. The platinum wire wound tightly around the YSZ tube (with Pt paste) was connected to the reference electrode (Ni + NiO). A solid electrolyte tube was assembled in an alumina crucible filled with the reference electrode. The reference electrode gas space of the alumina crucible was sealed with a ceramic stopper and alumina cement. The constructed cell assembly was placed into a silica tube with an upper brass head, and finally mounted in the tube of the resistance furnace.

Before the experiment took place, the silica tube was purged with purified Ar (99.999 vol.%, Air Products) to remove the oxygen traces. After that the temperature was slowly raised to a desired value of 1223 K, in which the reference electrodes were sintered before the start of each experiment. The samples were kept within the constant temperature zone of the furnace under constant argon flow during each experiment. The constant temperature was maintained within ± 1 K by use of temperature

controller Lumel type RE15 with a thyristor power unit.

The emf of the galvanic cell was continuously recorded by means of the digital Keithley 200 multimeter and the non-commercial computer program. The acquired cell signal controlling the temperature stability of the emf with high precision allows minimization of an experimental error. The emf values of the galvanic cell were measured in the range of temperature from 973 K to 1223 K for all three system sections $\text{Ag}_{0.25}\text{Sb}_{0.75}$, $\text{Ag}_{0.5}\text{Sb}_{0.5}$, $\text{Ag}_{0.75}\text{Sb}_{0.25}$. The measurements were carried out at increasing and decreasing temperature for several days. Some experiments have been carried out twice and the emf reproducibility was $\pm 2\%$.

At the beginning of an experiment, the possibility of an exchange reaction between SnO_2 and the alloy component should be ensured. For that reason, the equilibration experiments were performed at 1073 K and 1173 K. The pure metallic Sb lumps in SnO_2 ambient powder placed in alumina crucible were enclosed in an evacuated silica tube. After equilibration the metallic part was analyzed by energy dispersive x-ray spectrometry point and area analysis. The powder part of the sample was analyzed by the XRD method. No evidence of an exchange reaction was observed.

Calorimetric Technique

The MHTC 96 high-temperature drop calorimeter (Setaram, France) with a graphite tube resistance furnace was used. Its sensor was constructed in the shape of a thermopile of 20 Pt-PtRh10 thermocouples. The sensor temperature was controlled within ± 1 K.

Starting materials for all mixing enthalpy experiments included the silver wire (99.999 mass%), tin shots (99.998 mass%), and antimony lumps (99.9999 mass%) delivered by Alfa Aesar (Karlsruhe, Germany). The samples of pure silver or tin with masses of 45–70 mg were added from a manual dispenser to the liquid bath of a chosen starting composition of binary Sb-Sn and Ag-Sb alloys, respectively. At the end of each series the calorimeter was calibrated by three additions (approximately 20 mg each) of National Institute of Standards and Technology (NIST, Gaithersburg, USA) standard $\alpha\text{-Al}_2\text{O}_3$. Additionally, before each drop the dispenser temperature was controlled with the constantan-copper thermocouple.

The solvent bath of about 1 g of liquid binary alloy was placed in the calorimetric alumina crucibles (length 60 mm, OD 12 mm). This amount of solvent entirely covers the bottom of the crucible. At the beginning of every measurement the protection tube was evacuated three times repeatedly and flushed with high-purity argon (99.9999 vol.%, Air Products). To prevent the oxidation of the alloy samples an argon flow (approx. 30 ml/min) was maintained throughout the entire measurement. Weight loss

during measurements was negligible due to an insignificant difference between the total mass of the samples with crucibles before and after measurements.

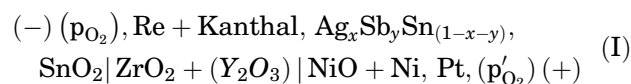
The system required ~ 30 min after the silver addition and ~ 25 min after the tin or $\alpha\text{-Al}_2\text{O}_3$ addition until the signal of the recorded heat effect had returned to the base line. The calorimetric measurements were performed for the Ag-Sb-Sn system along the $\text{Sb}_{0.5}\text{Sn}_{0.5}$ cross-section at 912 K and 1075 K, and along the $\text{Ag}_{0.75}\text{Sb}_{0.25}$ 3:1 cross-section at 1075 K. In order to check the reproducibility, the section $\text{Sb}_{0.5}\text{Sn}_{0.5}$ was measured twice at 912 K and three times at 1075 K.

Control of the entire equipment and data acquisition and evaluation was performed with Calisto software provided by the producer (Setaram, France). The recorded and integrated signals were used to calculate the resulting enthalpy of mixing, which are shown in Tables I, II, and III.

RESULTS

Emf Results

In order to determine tin activity in liquid Ag-Sb-Sn solutions, the emf, E , of the schematically presented electrochemical cell:

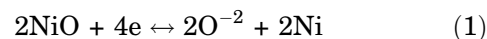


was recorded over the temperature range from 973 K to 1223 K for all three system sections with the ratio: $\text{Ag}_{0.25}\text{Sb}_{0.75}$, $\text{Ag}_{0.5}\text{Sb}_{0.5}$ and $\text{Ag}_{0.75}\text{Sb}_{0.25}$. The linear temperature function of the type: $E(T) = a + b \cdot T$ was applied to fit the obtained emf data by the least-squares method, and the results are presented in Table IV.

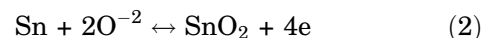
The emf values of the cell (I) for all three Ag:Sb sections are shown together with fitted lines in Fig. 2a–c, respectively.

The cell scheme is written in such a way that the right-hand side (RHS) electrode is positive. For galvanic cell I the electrode reactions are:

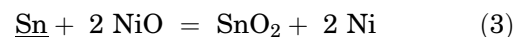
(a) at the RHS electrode:



(b) at the LHS electrode:



Consequently, the overall cell (I) reaction can be written in the form:



and the change of Gibbs free energy of the reversible reaction (3), $\Delta G_{(r)}$ can be derived as follows:

Table I. Partial and integral mixing enthalpies of liquid Ag-Sb-Sn alloys at 912 K, cross-section $\text{Sb}_{0.5}\text{Sn}_{0.5}$, standard state: liquid pure components

Composition			Partial enthalpy	Integral enthalpy
X_{Ag}	X_{Sb}	X_{Sn}	$\Delta\bar{H}_{\text{Ag}}^{\text{m}}/\text{J mol}^{-1}$	$\Delta H^{\text{m}}/\text{J mol}^{-1}$
Series I: cross-section $\text{Sb}_{0.5}\text{Sn}_{0.5}$, $T = 912$ K				
0.000	0.500	0.500	–	–1424
0.047	0.477	0.477	7222	–1020
0.091	0.455	0.455	6832	–655
0.132	0.434	0.434	4437	–424
0.171	0.414	0.414	5543	–155
0.209	0.396	0.396	3101	–9
0.243	0.378	0.378	1500	58
0.278	0.361	0.361	–295	42
0.309	0.346	0.346	1377	100
0.338	0.331	0.331	–405	78
0.366	0.317	0.317	–2016	–12
0.393	0.304	0.304	–2350	–109
0.418	0.291	0.291	–2405	–202
0.440	0.280	0.280	–2127	–278
0.462	0.269	0.269	–2203	–351
0.482	0.259	0.259	–3493	–470
0.501	0.249	0.249	–4739	–628
0.520	0.240	0.240	–6547	–848
Series II: cross-section $\text{Sb}_{0.5}\text{Sn}_{0.5}$, $T = 912$ K				
0.513	0.243	0.243	–2892	–512
0.525	0.238	0.238	–2692	–565
0.537	0.232	0.232	–5365	–686
0.549	0.226	0.226	–3494	–756
0.560	0.220	0.220	–4997	–866
0.572	0.214	0.214	–3590	–937
0.583	0.208	0.208	–3512	–1005
0.594	0.203	0.203	–5665	–1129
0.605	0.198	0.198	–5668	–1248
0.615	0.192	0.192	–4874	–1343
0.625	0.187	0.187	–4630	–1428
0.635	0.183	0.183	–5780	–1538
0.644	0.178	0.178	–6962	–1679
0.653	0.173	0.173	–6721	–1808
0.662	0.169	0.169	–4940	–1886
0.670	0.165	0.165	–7970	–2038
0.678	0.161	0.161	–7496	–2171

$$\Delta G_{(r)} = -4FE = \Delta G_{\text{f},\text{SnO}_2}^{\circ} - 2\Delta G_{\text{f},\text{NiO}}^{\circ} - RT \ln a_{\text{Sn}} \quad (4)$$

where: $\Delta G_{\text{f},\text{SnO}_2}^{\circ}$ and $\Delta G_{\text{f},\text{NiO}}^{\circ}$ are the standard Gibbs free energies of formation of the solid SnO_2 and NiO , respectively. The symbols F and R are the Faraday constant ($96,486 \text{ C mol}^{-1}$) and the gas constant ($8.314 \text{ J mol}^{-1} \text{ deg}^{-1}$), respectively.

If tin is in its pure liquid state ($a_{\text{Sn}} = 1.0$), then Eq. 4 takes the form:

$$-4FE^{\circ} = \Delta G_{\text{f},\text{SnO}_2}^{\circ} - 2\Delta G_{\text{f},\text{NiO}}^{\circ} \quad (5)$$

from which the change of Gibbs free energy of formation of pure solid SnO_2 was determined:

$$\Delta G_{\text{f},\text{SnO}_2}^{\circ} = -4FE^{\circ} + 2\Delta G_{\text{f},\text{NiO}}^{\circ} \quad (6)$$

Thus, using Eq. 6, the Gibbs free energy of formation of the solid SnO_2 , $\Delta G_{\text{f},\text{SnO}_2}^{\circ}$, can be determined from E° , measured as a function of temperature and compared with literature values to check emf experiment accuracy. In this work the necessary temperature function of $\Delta G_{\text{f},\text{NiO}}^{\circ}$ was taken from the work of Charette and Flengas.¹⁶

The separately measured temperature dependence of emf, ΔE_{corr} , for the platinum-Kanthal junction¹⁷:

$$\Delta E_{\text{corr}}(\text{V}) = 2.3636 \times 10^{-4} + 5.458 \times 10^{-7} T - 8.32 \times 10^{-9} T^2 \quad (7)$$

was added to all recorded experimental emf values of galvanic cells as a thermoelectric correction. As

Table II. Partial and integral mixing enthalpies of liquid Ag-Sb-Sn alloys at 1075 K, along $\text{Sb}_{0.5}\text{Sn}_{0.5}$ cross-section, (standard state: liquid pure components)

Composition			Partial enthalpy	Integral enthalpy
X_{Ag}	X_{Sb}	X_{Sn}	$\Delta\bar{H}_{\text{Ag}}^{\text{m}}/\text{J mol}^{-1}$	$\Delta H^{\text{m}}/\text{J mol}^{-1}$
Series I: cross-section $\text{Sb}_{0.5}\text{Sn}_{0.5}$, $T = 1075$ K				
0.000	0.500	0.500	—	−1424
0.062	0.469	0.469	3264	−1133
0.118	0.441	0.441	7347	−624
0.170	0.415	0.415	5624	−260
0.220	0.390	0.390	2457	−96
0.266	0.367	0.367	1982	27
0.310	0.345	0.345	1427	110
0.350	0.325	0.325	−1061	41
0.386	0.307	0.307	−1618	−54
0.422	0.289	0.289	−3828	−267
0.452	0.274	0.274	−4056	−471
0.482	0.259	0.259	−4612	−688
0.508	0.246	0.246	−4070	−856
0.532	0.234	0.234	−4541	−1038
0.554	0.223	0.223	−4889	−1223
0.574	0.213	0.213	−6489	−1466
0.594	0.203	0.203	−6295	−1683
0.612	0.194	0.194	−6057	−1872
Series II: cross-section $\text{Sb}_{0.5}\text{Sn}_{0.5}$, $T = 1075$ K				
0.000	0.500	0.500	—	−1424
0.060	0.470	0.470	5025	−1029
0.120	0.440	0.440	5442	−624
0.174	0.413	0.413	3428	−376
0.226	0.387	0.387	2459	−197
0.272	0.364	0.364	956	−128
0.314	0.343	0.343	2783	45
0.354	0.323	0.323	−1594	−49
0.390	0.305	0.305	−2981	−210
0.424	0.288	0.288	−2399	−331
0.454	0.273	0.273	−4657	−561
0.482	0.259	0.259	−2618	−668
0.508	0.246	0.246	−4170	−842
0.532	0.234	0.234	−3136	−954
0.554	0.223	0.223	−4795	−1135
0.574	0.213	0.213	−4291	−1279
0.594	0.203	0.203	−4379	−1415
0.610	0.195	0.195	−5204	−1578
Series III: cross-section $\text{Sb}_{0.5}\text{Sn}_{0.5}$, $T = 1075$ K				
0.588	0.206	0.206	−7942	−1647
0.600	0.200	0.200	−4127	−1719
0.612	0.194	0.194	−4449	−1802
0.624	0.188	0.188	−5577	−1918
0.636	0.182	0.182	−6201	−2053
0.646	0.177	0.177	−4512	−2130
0.658	0.171	0.171	−6281	−2261
0.668	0.166	0.166	−6523	−2393
0.678	0.161	0.161	−5887	−2499
0.688	0.156	0.156	−6158	−2609
0.698	0.151	0.151	−6755	−2730
0.706	0.147	0.147	−6680	−2844
0.714	0.143	0.143	−6336	−2943
0.722	0.139	0.139	−5104	−3003
0.730	0.135	0.135	−4167	−3035
0.738	0.131	0.131	−4771	−3084

Table III. Partial and integral mixing enthalpies of liquid Ag-Sb-Sn alloys at 1075 K, cross-section $\text{Ag}_{0.75}\text{Sb}_{0.25}$, (standard state: liquid pure components)

Composition			Partial enthalpy	Integral enthalpy
X_{Ag}	X_{Sb}	X_{Sn}	$\Delta\bar{H}_{\text{Sn}}^{\text{m}}/\text{J mol}^{-1}$	$\Delta H^{\text{m}}/\text{J mol}^{-1}$
Series I: cross-section $\text{Ag}_{0.75}\text{Sb}_{0.25}$, $T = 1075$ K				
0.750	0.250	0.000	–	–2663
0.717	0.238	0.045	4788	–2326
0.683	0.227	0.090	4796	–1992
0.652	0.217	0.131	5182	–1667
0.623	0.208	0.169	3016	–1463
0.597	0.199	0.204	4578	–1207
0.572	0.190	0.238	4298	–973
0.548	0.182	0.270	3984	–768
0.526	0.175	0.299	3644	–592
0.506	0.168	0.326	5183	–366
0.486	0.162	0.352	5672	–135
0.468	0.156	0.376	5055	58
0.451	0.150	0.399	3647	191
0.433	0.145	0.422	2753	286
0.418	0.139	0.443	2516	368
0.404	0.134	0.462	2417	440
0.389	0.130	0.481	2311	505
0.376	0.125	0.499	1940	556
0.363	0.121	0.516	2235	613
0.350	0.117	0.533	2088	663
0.339	0.113	0.548	2766	732

Table IV. Temperature-dependent emf, $E(T)$, of cell (I) of three different cross-sections of Ag-Sb-Sn system

X_{Sn}	$E(T)/\text{V} = a + b T/\text{K}$		
	$\text{Ag}_{0.25}\text{Sb}_{0.75}$	$\text{Ag}_{0.5}\text{Sb}_{0.5}$	$\text{Ag}_{0.75}\text{Sb}_{0.25}$
1.0	$0.26256 - 8.09 \times 10^{-5} T \pm 0.00212$	–	–
0.8	$0.24727 - 7.47 \times 10^{-5} T \pm 0.00057$	$0.26125 - 8.56 \times 10^{-5} T \pm 0.00043$	$0.26457 - 8.87 \times 10^{-5} T \pm 0.00081$
0.7	$0.24666 - 7.84 \times 10^{-5} T \pm 0.00058$	$0.25428 - 8.28 \times 10^{-5} T \pm 0.00086$	$0.25657 - 8.49 \times 10^{-5} T \pm 0.00084$
0.6	$0.26055 - 9.49 \times 10^{-5} T \pm 0.00026$	$0.24900 - 8.31 \times 10^{-5} T \pm 0.00079$	$0.25297 - 8.59 \times 10^{-5} T \pm 0.00084$
0.5	$0.23286 - 7.54 \times 10^{-5} T \pm 0.00069$	$0.25479 - 9.22 \times 10^{-5} T \pm 0.00076$	$0.23750 - 7.84 \times 10^{-5} T \pm 0.00093$
0.4	$0.23075 - 7.97 \times 10^{-5} T \pm 0.00101$	$0.24675 - 9.02 \times 10^{-5} T \pm 0.00075$	$0.23875 - 8.50 \times 10^{-5} T \pm 0.00050$
0.3	$0.22604 - 8.41 \times 10^{-5} T \pm 0.00126$	$0.26446 - 1.146 \times 10^{-4} T \pm 0.00059$	$0.25329 - 1.041 \times 10^{-4} T \pm 0.00079$
0.2	$0.18850 - 6.62 \times 10^{-5} T \pm 0.00096$	$0.26026 - 1.215 \times 10^{-4} T \pm 0.00056$	$0.27230 - 1.306 \times 10^{-4} T \pm 0.00032$

the Kanthal-Re joint is in the constant temperature zone of the furnace, the thermoelectric force due to the Kanthal-Re junction may be neglected.

At the beginning, to test the assembly and to obtain the reference state to study tin activity, the Gibbs free energy of formation of SnO_2 was derived from the experimental data according to Eq. 6. The obtained values of Gibbs free energy yielded the following temperature dependence:

$$\Delta G_{\text{f},\text{SnO}_2}^{\circ} = -568650.8 + 201.01 T (\pm 2150 \text{ J mol}^{-1}), \quad (8)$$

which within the range of experimental error is in good agreement with a set of literature data.^{18–24}

Next, for liquid tin solutions, when $a_{\text{Sn}} \neq 1$, the expression relating tin activity can be determined from measured emf values by combining Eqs. 4 and 5:

$$\ln a_{\text{Sn}} = \frac{4F}{RT} (E - E^0) \quad (9)$$

where E is a function of temperature and the alloy composition.

The activity of tin in the Ag-Sb-Sn liquid alloys was calculated for the three system sections $\text{Ag}_{0.75}\text{Sb}_{0.25}$, $\text{Ag}_{0.5}\text{Sb}_{0.5}$, and $\text{Ag}_{0.25}\text{Sb}_{0.75}$ (Eq. 9 at two different temperatures, 1073 K and 1223 K) and the results are shown in Fig. 3a–c, respectively. Uncertainty limits in the activity values can be derived from those in the emf values.

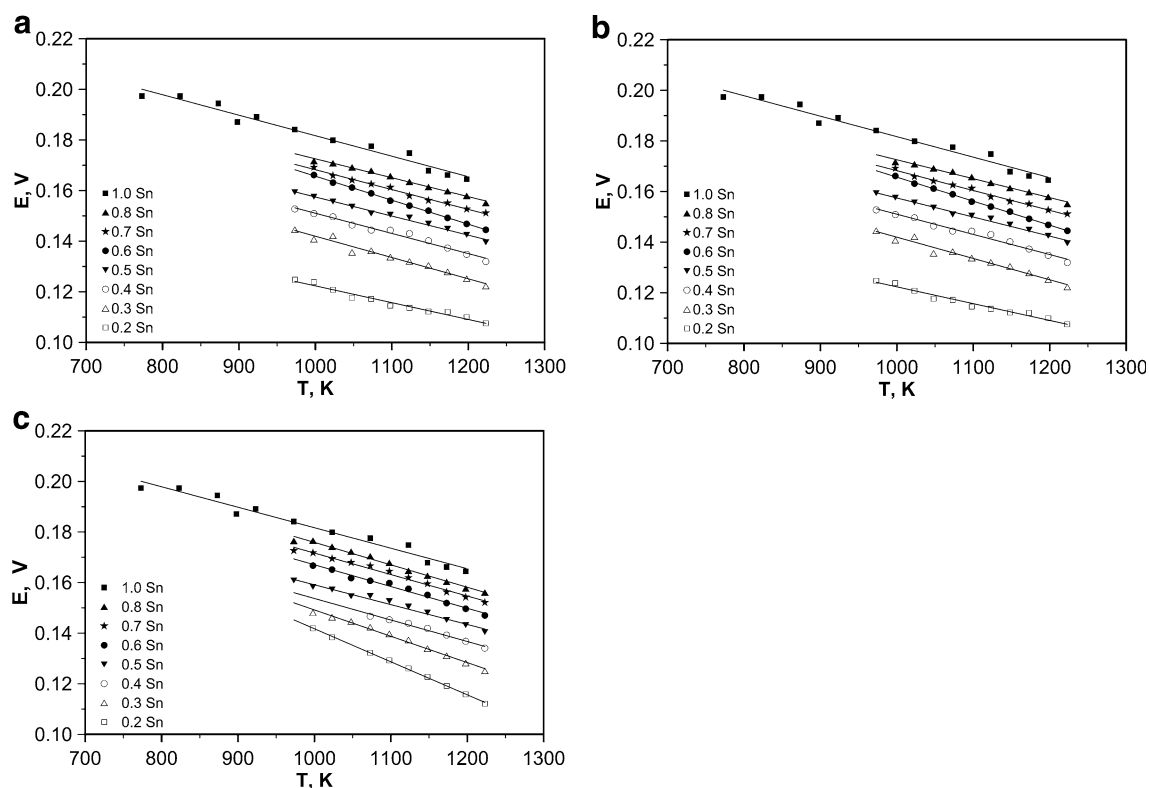


Fig. 2. Plot of the cell (I) emf vs. temperature along the Ag-Sb-Sn system cross-sections (a) $\text{Ag}_{0.25}\text{Sb}_{0.75}$, (b) $\text{Ag}_{0.5}\text{Sb}_{0.5}$, (c) $\text{Ag}_{0.75}\text{Sb}_{0.25}$.

Tin activity of liquid ternary alloys of the Ag-Sb-Sn system shows negative deviation from the Raoult's law for all three experimental isopleths, and the temperature dependence of the activity is small. The deviation tends to decrease with temperature increase, an effect that is consistent with Raoult's law fulfillment at elevated temperatures.

Calorimetric Results

The enthalpy measured in i th drops of element A (integrated heat flow at constant pressure), $\Delta H_{A,i}^{\text{Reaction}}$, is expressed by the relationship:

$$\Delta H_{A,i}^{\text{Reaction}} = (\Delta H_{A,i}^{\text{Signal}} \cdot C) - (\Delta H_{A,i}^{T_D \rightarrow T_M} \cdot n_{A,i}) \quad (A = \text{Ag or Sn}) \quad (10)$$

where $n_{A,i}$ is the number of moles of metal A added in i -th drops. $\Delta H_{A,i}^{\text{Signal}}$ refers to the heat effect of a single " i " drop of A (tin or silver) to the bath and C is the calorimeter constant. The enthalpy difference, $\Delta H_{A,i}^{T_D \rightarrow T_M}$, is the enthalpy change of 1 mol of A (Ag or Sn) from the solid state at drop temperature T_D (in Kelvins) to the liquid state at the temperature of the bath T_M , in the respective measurement " i ". The values of $\Delta H_{A,i}^{T_D \rightarrow T_M}$ were calculated using polynomials from the SGTE* Pure database.²⁵

The added number of moles of A was rather small in comparison to the number of moles of the ternary alloy, and thus the heat effect of single drop of A could be related only to $n_{A,i}$ moles without a significant change in the global composition. Therefore, the partial molar enthalpy of mixing can be derived directly as:

$$\Delta \bar{H}_{A,i}^m = \Delta H_{A,i}^{\text{Reaction}} / n_{A,i} \quad (A = \text{Ag or Sn, respectively}) \quad (11)$$

For measurements starting with n_0 mol of the bath of liquid binary alloy, the mixing enthalpy of the binary bath $n_0 \cdot \Delta^0 H^m$ should be taken into account. So, after i drops, the total contribution to the enthalpy of mixing due to adding A into the binary bath has this form:

$$\Delta H_i^m = n_0 \cdot \Delta^0 H^m + \sum_i \Delta H_{A,i}^{\text{Reaction}} \quad (12)$$

The integral molar enthalpy of mixing, ΔH^m , was calculated by summarizing the respective reaction enthalpies and division by the total molar amount of the liquid Ag-Sb-Sn alloys:

$$\Delta H^m = \Delta H_i^m / \sum_j n_j \quad (j = \text{Ag, Sb, Sn}) \quad (13)$$

*Scientific Group Thermodata Europe.

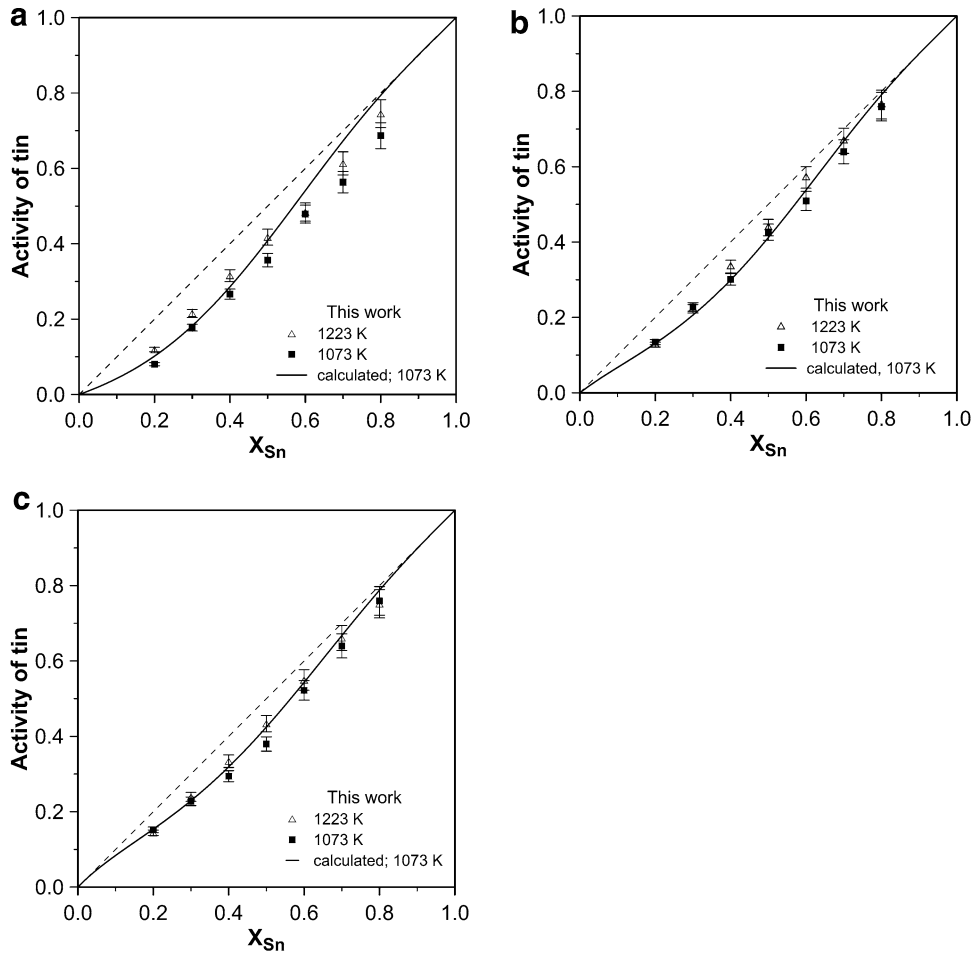


Fig. 3. Plot of the activity vs. tin mol fraction in liquid alloys at temperatures 1073 K and 1223 K for the cross-sections: (a) $\text{Ag}_{0.25}\text{Sb}_{0.75}$, (b) $\text{Ag}_{0.5}\text{Sb}_{0.5}$, (c) $\text{Ag}_{0.75}\text{Sb}_{0.25}$.

Table V. The optimized ternary excess parameters of Ag-Sb-Sn liquid solution in the Redlich-Kister-Muggianu model. The parameters of the liquid phase of binary systems were enclosed²⁶

Binary and ternary parameters	Formula	Reference
Liquid, sublattice model: (Ag, Sb, Sn)		
${}^0L_{\text{Ag,Sb}}$	$-964 - 7.988 T$	26
${}^1L_{\text{Ag,Sb}}$	$-21481 + 7.174 T$	
${}^2L_{\text{Ag,Sb}}$	-9992	
${}^0L_{\text{Ag,Sn}}$	$-3177 - 10.161 T + 0.381 T \ln(T)$	
${}^1L_{\text{Ag,Sn}}$	$-16782 + 2.065 T + 0.437 T \ln(T)$	
${}^2L_{\text{Ag,Sn}}$	$+3190 - 107.095 T + 13.955 T \ln(T)$	
${}^0L_{\text{Sb,Sn}}$	$-5695.1 - 1.709 T$	
${}^1L_{\text{Sb,Sn}}$	783	
${}^2L_{\text{Sb,Sn}}$	1841	
${}^0L_{\text{Ag,Sb,Sn}}$	$+93776 + 18.116 T$	This work
${}^1L_{\text{Ag,Sb,Sn}}$	$-83050 + 31.993 T$	
${}^2L_{\text{Ag,Sb,Sn}}$	$+87255 - 110.610 T$	

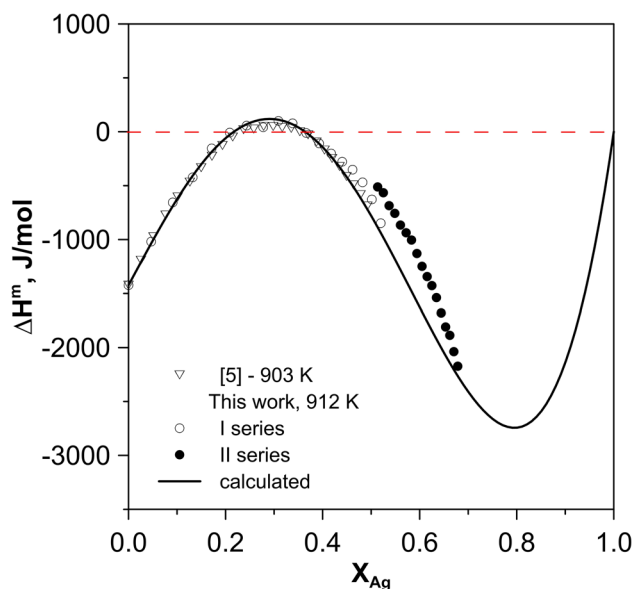


Fig. 4. Concentration dependence of integral molar enthalpy of mixing of liquid Ag-Sb-Sn alloys along the $\text{Sb}_{0.5}\text{Sn}_{0.5}$ section at 912 K. The presented experimental values are compared with those of Li et al.⁵ at 903 K.

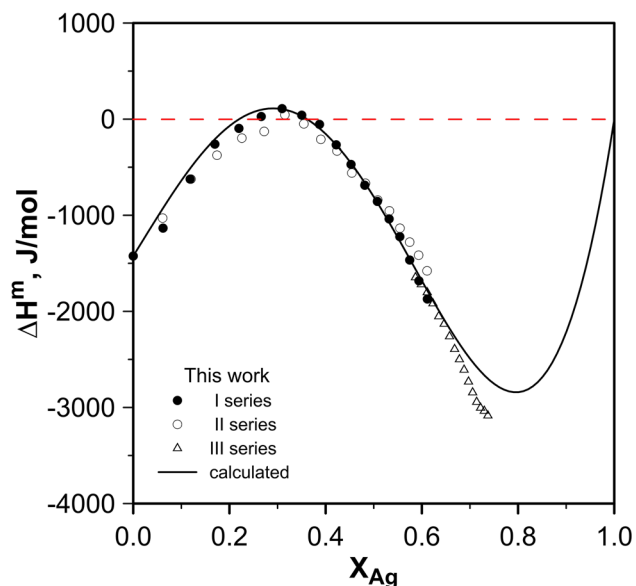


Fig. 5. Integral molar enthalpy of mixing of liquid Ag-Sb-Sn alloys along the $\text{Sb}_{0.5}\text{Sn}_{0.5}$ section at 1075 K. The experimental values obtained in this work are superimposed.

The binary starting value for respective sections in the ternary system was calculated from the COST MP0602** database²⁶ (Table V).

The integral molar mixing enthalpies of liquid Ag-Sb-Sn alloys obtained in the separate experiments

**COST MP0602—Advanced Solder Materials for High Temperature Application (HISOLD) COST Action; http://www.cost.eu/COST_Actions/mpns/HISOLD.

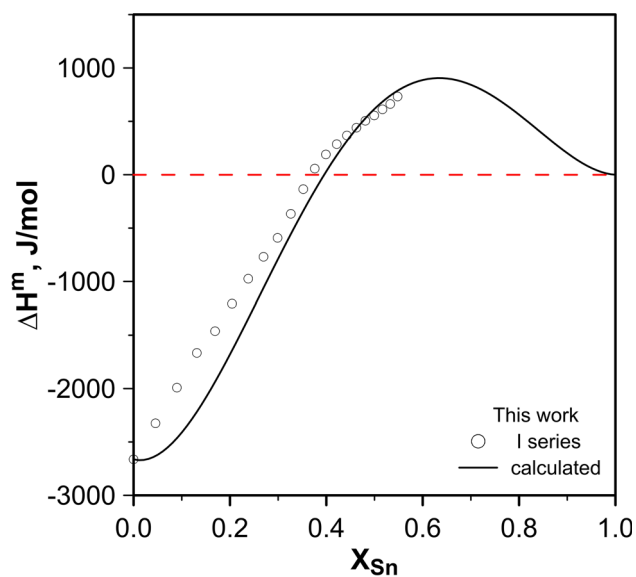


Fig. 6. Integral molar enthalpy of mixing of liquid Ag-Sb-Sn alloys along the $\text{Ag}_{0.75}\text{Sb}_{0.25}$ section at 1075 K. The presented experimental values are superimposed.

are presented in Tables I, II, and III and in the Figs. 4, 5, and 6 (reference state is pure liquid component). These tables also provide information about the mole fraction of tin and silver, and their partial molar enthalpies, respectively.

Generally, an uncertainty of calorimetric measurements depends mainly on the construction of the calorimeter, calibration procedure, signal integration method, and “chemical errors”, e.g. an incomplete reaction of dissolution or presence of impurities. Considering calibration measurements done by dropping NIST standard sapphire, the standard deviation for the MHTC 96 instrument (Setaram, France) was estimated to be less than $\pm 1.5\%$. The overall experimental error connected with the MHTC 96 calorimeter is $\pm 250 \text{ J mol}^{-1}$.

To test the calorimeter assembly, the results obtained from experiments at 912 K for increasing Ag concentration along the section $\text{Sb}_{0.50}\text{Sn}_{0.50}$ (Ag pieces were dropped into an Sb-Sn liquid bath) were compared with the experimental data of Li et al.⁵ Along the studied $\text{Sb}_{0.50}\text{Sn}_{0.50}$ section, the negative values of integral mixing enthalpy were observed with a maximum (near 0 J/mole) at around 30 at.% for the two experimental temperatures. The values obtained from different runs for the same temperature and composition are similar and were consistent with the experimental data of Li et al.⁵ (Fig. 4). The mixing enthalpy values for the binary bath alloys were also calculated from the COST MP0602 database.^{3,26}

THERMODYNAMIC DESCRIPTION OF THE LIQUID PHASE

During the optimization of the Ag-Sb-Sn system the substitutional solution model was selected for

thermodynamic description of the liquid phase (L). In this model the Gibbs energy per mole of atoms is expressed as:

$$G_m^L(T) = {}^{\text{ref}}G_m^L + {}^{\text{id}}G_m^L + {}^{\text{ex}}G_m^L \quad (14)$$

$${}^{\text{ref}}G_m^L = X_{\text{Ag}}^0 G_{\text{Ag}}^L(T) + X_{\text{Sb}}^0 G_{\text{Sb}}^L(T) + X_{\text{Sn}}^0 G_{\text{Sn}}^L(T) \quad (15)$$

$${}^{\text{id}}G_m^L = RT(X_{\text{Ag}} \ln(X_{\text{Ag}}) + X_{\text{Sb}} \ln(X_{\text{Sb}}) + X_{\text{Sn}} \ln(X_{\text{Sn}})) \quad (16)$$

The thermodynamic properties of the ternary liquid solutions were estimated from the assessed description of the binary constituent systems by the Muggianu method^{27,28}:

$$\begin{aligned} {}^{\text{ex}}G_m^L = & X_{\text{Ag}}X_{\text{Sb}} \sum_i {}^iL_{\text{Ag,Sb}}^L (X_{\text{Ag}} - X_{\text{Sb}})^i \\ & + X_{\text{Ag}}X_{\text{Sn}} \sum_i {}^iL_{\text{Ag,Sn}}^L (X_{\text{Ag}} - X_{\text{Sn}})^i \\ & + X_{\text{Sb}}X_{\text{Sn}} \sum_i {}^iL_{\text{Sb,Sn}}^L (X_{\text{Sb}} - X_{\text{Sn}})^i \\ & + X_{\text{Ag}}X_{\text{Sb}}X_{\text{Sn}} {}^{\text{ter}}L_{\text{Ag,Sb,Sn}}^L \end{aligned} \quad (17)$$

where ${}^0G_i^L$ denotes the Gibbs energy of the pure liquid element i ($i = \text{Ag}, \text{Sb}, \text{Sn}$).

In the present work, the data for the pure elements were taken from the compilation by Dinsdale.²⁵ ${}^{\text{ref}}G_m^L$ refers to the mixture of the pure liquid elements in the liquid phase at temperature T , ${}^{\text{id}}G_m^L$ is the Gibbs energy contribution resulting from the ideal entropy of mixing, and ${}^{\text{ex}}G_m^L$ is the excess Gibbs energy of mixing.

The L_{ij} parameters in Eq. 17, often referred to as the Redlich–Kister equation,²⁷ are the interaction parameters between the species given by the subscript (i and j), and may be temperature dependent.

The use of the first three terms of Eq. 17 gives the thermodynamic description of ternary phases from respective binaries (“binary formalism”) as a first approximation of the ternary system. The only possibility to refine the calculated topology of the ternary system according to measured thermodynamic data is to use the ternary interaction parameters, which should be optimized according to experimental data obtained for the ternary system.

The ternary interaction parameter ${}^{\text{ter}}L_{\text{Ag,Sb,Sn}}^L$ is composition dependent and has the following form:

$$\begin{aligned} {}^{\text{ter}}L_{\text{Ag,Sb,Sn}}^L = & X_{\text{Ag}}^0 L_{\text{Ag,Sb,Sn}}^L + X_{\text{Sb}}^1 L_{\text{Ag,Sb,Sn}}^L \\ & + X_{\text{Sn}}^2 L_{\text{Ag,Sb,Sn}}^L \end{aligned} \quad (18)$$

where: ${}^iL_{\text{Ag,Sb,Sn}}^L$ are attached in Table V.

DISCUSSION

Thermodynamic properties of the liquid Ag-Sb-Sn solutions were determined using solid oxide galvanic cells with the YSZ electrolyte. The experiments were carried out in the temperature range from 973 K to 1223 K, and along three cross-sections of the ternary system. Recorded emf values were repeated during experiments on cooling and heating cycles, which proved that the cells worked reversibly for about a week. Also, a small current passed through the cell at constant temperature did not change emf equilibrium value, which usually returned after disturbance to the initial value after several minutes.

Activities of tin were determined for the first time over the whole concentration range in Ag-Sb-Sn ternary liquid solutions. They show slight negative deviation from the ideal solution along all three investigated cross-sections. No other experimental data concerning activities in this ternary liquid system were found in the literature, so direct comparison of our data with the information from different sources is impossible. Therefore, activities in respective binary systems were analyzed since they are the boundary limits for the activity changes in the considered ternary system.

As far as the Ag-Sb system is concerned there are several studies that provided activity values for both components in this system. Nozaki et al.²⁹ as well as Vechter et al.³⁰ used emf cells with the molten salts electrolyte, from which the activity of silver was derived. The activity of antimony was determined by the vapor pressure method by Hino et al.³¹ and also by Krzyżak and Fitzner,³² who used emf cells with the solid electrolyte. All these results show negative deviation from Raoult’s Law, with increasing deviation for antimony as X_{Ag} approaches pure silver.

The system of silver with tin was investigated a number of times. Chowdhury and Ghosh,³³ Kubaschewski and Alcock,³⁴ Seetharaman and Staffansson,³⁵ Iwase et al.³⁶ and Kameda et al.³⁷ demonstrated that the activity of tin exhibits negative deviation from Raoult’s Law, which is almost insignificant for tin-rich alloys and deviates visibly for X_{Ag} approaching pure silver.

Finally, the data available for the Sb-Sn system were recently discussed by Jendrzeczyk-Handzlik and Fitzner.³⁸ Activities in this liquid system show slight negative deviation from ideality over the whole concentration range.

The results discussed above indicate that negative deviation of tin activities found in the ternary system is compatible with the information existing for respective binaries. However, measured enthalpy values indicate different trend (Figs. 4, 5 and 6). They show the change from negative to positive deviation depending on the concentration range. This kind of dependence was also recently detected by Li et al.,⁵ who measured enthalpy of mixing of Ag-Sb-Sn along five sections at three

different temperatures (803 K, 873 K, and 903 K) using a high-temperature Calvet type calorimeter. To get a consistent description of the thermodynamic properties of the liquid phase, commercial software^{39,40} was used. Ternary excess coefficients of the Redlich–Kister–Muggianu model were optimized for the liquid phase using our own experimental data, and they are gathered in Table V. The calculated results fit the experimental data very well within the range of experimental scatter. The enthalpy data show a characteristic s-shape along all three cross-sections, which implies the possibility of clustering atoms within a certain concentration range.

The comparison of the results obtained with this model with the data of Li et al.⁵ along two cross-

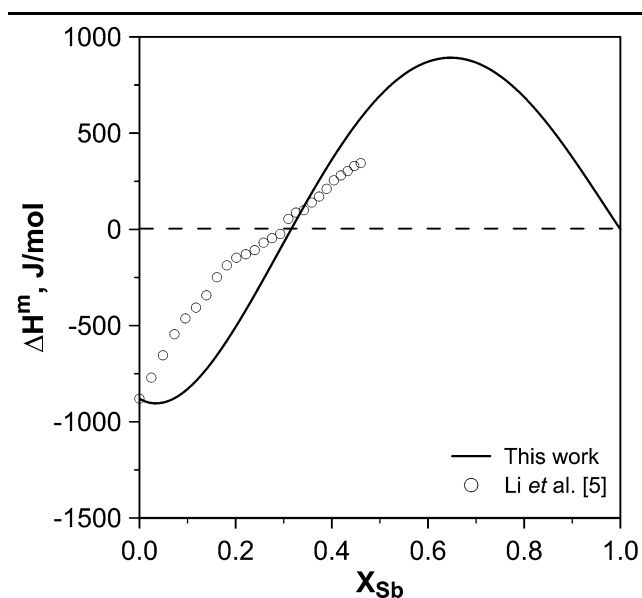


Fig. 7. Integral molar enthalpy of mixing of liquid Ag-Sb-Sn alloys along the $\text{Ag}_{0.5}\text{Sn}_{0.5}$ section at 912 K. The enthalpy values of Li et al.⁵ were superimposed.

sections (Figs. 5 and 7) is also given as an example. It is seen that the model with optimized parameters given in Table V reproduces those results very well, though these experiments were not taken into account during the optimization procedure. A reliable description of the thermodynamic properties of the liquid phase may aid in the explanation of the apparent contradiction between activity and enthalpy concentration behavior.

Calculated iso-enthalpy, ΔH_m , seen as curves in the ternary system shown in Fig. 8a, demonstrates the existence of possible segregation region and clustering region within the melt depending on the concentration range. However, calculated iso-entropy, ΔS_m , seen as curves shown in Fig. 8b, indicates positive values over all concentration ranges. It is clear that $-T\Delta S_m$ must be responsible for leveling the ΔH_m influence on Gibbs free energy of mixing, which results in the observed activity concentration dependence.

CONCLUSIONS

The thermodynamic properties of liquid Ag-Sb-Sn alloys were determined by use of a drop solution calorimetry and emf method. Galvanic cells with zirconia solid electrolyte were used and the experiments were carried out along $\text{Ag}_{0.25}\text{Sb}_{0.75}$, $\text{Ag}_{0.5}\text{Sb}_{0.5}$, and $\text{Ag}_{0.75}\text{Sb}_{0.25}$ sections in the temperature range 973–1223 K. The activity of tin was determined for the first time in this ternary system. Tin activity data exhibits the negative deviation from Raoult's law for all three isopleths over the entire composition range.

A set of mixing enthalpies for the Ag-Sb-Sn ternary system measured at 912 K and 1075 K by use of a high-temperature Calvet-type calorimeter was also presented. The ternary liquid alloys were investigated along two different cross-sections: $\text{Sb}_{0.50}\text{Sn}_{0.50}$, and $\text{Ag}_{0.75}\text{Sb}_{0.25}$. No significant temperature dependence of the mixing enthalpy can be

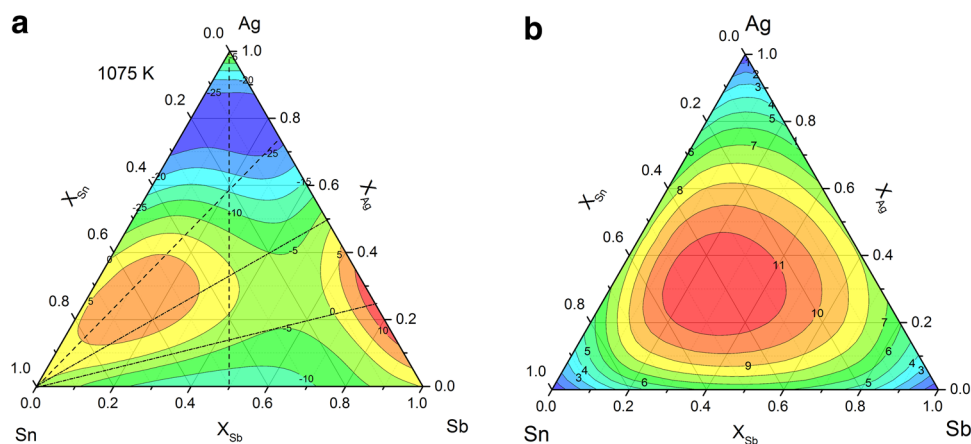


Fig. 8. (a) The iso-enthalpy of mixing (in 10^2 J/mol) calculated at 1075 K for the liquid phase using the geometrical model of Muggianu et al.²⁷ The experimental enthalpy isopleths are denoted by dash lines together with isopleths for which tin activity was determined (dash-dot line). (b) The iso-entropy of mixing of the liquid solution (in $\text{J mol}^{-1} \text{K}^{-1}$) determined at 1075 K.

observed in the considered temperature range. Obtained data are consistent (Figs. 5 and 7) and agree very well with the data of Li et al.⁵ in the frame of the experimental error.

Experimental data sets were used to find the ternary interaction parameters of the Redlich–Kister–Muggianu model of the substitutional solution.^{27,28} The optimized model parameters are given in Table V. The calculated tin activity values fit the experimental results very well. Also, the calculated values of the enthalpy of mixing are in good agreement with the measured values for both sections and both temperatures. Additionally, it should be emphasized that the calculated enthalpy and entropy isolines allow us to explain that the S-shape concentration dependence of enthalpy may exist while the components activity dependence is negative in all concentration ranges.

The results of this work will be subsequently used in the optimization of phase equilibria in the Ag–Sb–Sn system.

ACKNOWLEDGEMENTS

This work was supported by the State Committee for Scientific Research at AGH University Science and Technology, Faculty of Non-Ferrous Metals in Krakow, Poland under Grant Number 129/N-COST/2008.

OPEN ACCESS

This article is distributed under the terms of the Creative Commons Attribution 4.0 International License (<http://creativecommons.org/licenses/by/4.0/>), which permits unrestricted use, distribution, and reproduction in any medium, provided you give appropriate credit to the original author(s) and the source, provide a link to the Creative Commons license, and indicate if changes were made.

REFERENCES

1. R.W. Neu, D.T. Scott, and M.W. Woodmansee, *J. Electron. Packag.* 123, 238 (2001).
2. D.B. Masson and B.K. Kirkpatrick, *J. Electron. Mater.* 15, 349 (1986).
3. A. Kroupa, A.T. Dinsdale, A. Watson, J. Vrestal, J. Vizdal, and A. Zemanova, *JOM* 59, 20 (2007).
4. B. Gather, P. Schroter, and R. Blachnik, *Z. Metallkd.* 78, 280 (1987).
5. D. Li, S. Delsante, A. Watson, and G. Borzone, *J. Electron. Mater.* 41, 67 (2011).
6. S.W. Chen, P.Y. Chen, C.N. Chiu, Y.C. Huang, and C.H. Wang, *Metall. Mater. Trans. A* 39, 3191 (2008).
7. C.S. Chen and Y.L. Lee, *J. Natl. Sci. People's Univ. North-East China* 33 (1957).
8. J. Zheng, *Acta Phys. Sinica* 14, 393 (1958).
9. P.J. Oberndorff, A.A. Kodentsov, V. Vuorinen, J.K. Kivilahti, and F.J.J. van Loo, *Ber. Bunsenges. Phys. Chem.* 102, 1321 (1998).
10. C.Y. Lin, C. Lee, X. Liu, and Y.W. Yen, *Intermetallics* 16, 230 (2008).
11. C.S. Oh, J.H. Shim, B.J. Lee, and D.N. Lee, *J. Alloys Compd.* 238, 155 (1996).
12. S.W. Chen, C.C. Chen, W. Gierlotka, A.R. Zi, P.Y. Chen, and H.J. Wu, *J. Electron. Mater.* 37, 992 (2008).
13. R. Schmid-Fetzer, L. Rokhlin, E. Lysova, and M. Zinkevich, in *Silver-antimony-tin. Thermodynamic Properties Ternary Alloy Systems: Phase Diagrams, Crystallographic and Thermodynamic Data Critically Evaluated by MSIT. Noble Metal Systems. Selected Systems from Ag-Al-Zn to Rh-Ru-Sc*, Part 11B, eds. G. Effenberg, S. Ilyenko (Berlin, Springer, 2006) p. 181.
14. W. Gierlotka, Y.-C. Huang, and S.-W. Chen, *Metall. Mater. Trans. A* 39, 3199 (2008).
15. T.B. Massalski, H. Okamoto, P.R. Subramanian, and L. Kacprzak, *Binary Alloy Phase Diagrams*, 2nd ed. (Materials Park: ASM International, 1996), p. 3304.
16. G.G. Charette and S.N. Flengas, *J. Electrochem. Soc.* 115, 796 (1968).
17. J. Nyk and B. Onderka, *Monatsh. Chem.* 143, 1219 (2012).
18. T.N. Belford and C.B. Alcock, *Trans. Faraday Soc.* 61, 443 (1965).
19. G. Petot-Ervas, R. Farhi, and C. Petot, *J. Chem. Thermodyn.* 7, 1131 (1975).
20. S. Seetharaman and L.I. Staffansson, *Scand. J. Metall.* 6, 143 (1977).
21. T. Oishi, T. Hiruma, and J. Moriyama, *Nippon Kinzoku Gakkaishi* 36, 481 (1972).
22. Y. Matsushita and K. Goto, in *Thermodynamics*, ed. H. Schmalzried, Vol. I, (IAEA, Vienna, 1966) p. 111.
23. M.J. Bannister, *J. Chem. Thermodyn.* 18, 455 (1986).
24. C. Mallika, A.M.E.S. Raj, K.S. Nagaraja, and O.M. Sreedharan, *Thermochim. Acta* 371, 95 (2001).
25. A.T. Dinsdale, *Calphad* 15, 317 (1991).
26. A. Kroupa, A. Dinsdale, A. Watson, J.J. Vřešťál, A. Zemanova, and P. Broz, *J. Min. Metall. Sect. B-Metall. B* 48, 339 (2012).
27. O. Redlich and A.T. Kister, *Ind. Eng. Chem. Res.* 40, 345 (1948).
28. M. Muggianu, M. Gambino, and J.-P. Bros, *J. Chim. Phys.* 72, 83 (1975).
29. T. Nozaki, M. Shimoji, and K. Niwa, *Ber. Bunsenges.* 70, 207 (1966).
30. A.A. Vecher and Y.I. Gerasimov, *Doklady Acad. Sci. SSSR* 134, 863 (1961).
31. M. Hino, T. Azakami, and M. Kameda, *J. Japan Inst. Met.* 39, 1175 (1975).
32. A. Krzyżak and K. Fitzner, *Thermochim. Acta* 414, 115 (2004).
33. P.J.R. Chowdhury and A. Ghosh, *Metall. Mater. Trans. B* 2, 2171 (1971).
34. P. Kubaschewski and C.B. Alcock, *J. Chem. Thermodyn.* 4, 259 (1972).
35. S. Seetharaman and L.I. Staffansson, *Chem. Scr.* 10, 61 (1976).
36. M. Iwase, M. Yasuda, S. Miki, and T. Mohri, *Trans. JIM* 19, 654 (1978).
37. K. Kameda, Y. Yoshida, and S. Sakairi, *J. Japan Inst. Met.* 44, 858 (1980).
38. D. Jendrzeczyk-Handzlik and K. Fitzner, *J. Chem. Thermodyn.* 85, 86 (2015).
39. J.O. Andersson, T. Helander, L. Höglund, P.F. Shi, and B. Sundman, *Calphad* 26, 273 (2002).
40. W. Cao, S.-L. Chen, F. Zhang, K. Wu, Y. Yang, Y.A. Chang, R. Schmid-Fetzer, and W.A. Oates, *Calphad* 33, 328 (2009).